DOI: http://dx.doi.org/10.22104/ijhfc.2017.2392.1151

Iranian Journal of Hydrogen & Fuel Cell 2(2017) 103-118

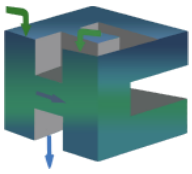

Iranian Journal of Hydrogen & Fuel Cell

IJHFC

Journal homepage://ijhfc.irost.ir

Simulation of a solid oxide fuel cell with external steam methane reforming and bypass

H. A. Ozgoli, A. Allahyari*

Department of Mechanical Engineering, Iranian Research Organization for Science and Technology (IROST), Tehran, Iran

Article Information

Article History:

Received:
07 Aug 2017
Received in revised form:
10 Sep 2017
Accepted:
12 Sep 2017

Keywords

Solid oxide fuel cell
Methane steam reforming
Energy efficiency
Heat recovery

Abstract

Fuel flexibility is a significant advantage of solid oxide fuel cells (SOFCs) and can be attributed to their high operating temperature. The eligibility of a combined heat and power (CHP) system has been investigated as a new power generation method, in this study. Natural gas fueled SOFC power systems employing methane steam reforming (MSR) yield electrical conversion efficiencies exceeding 50% and may become a viable alternative for distributed generation in Iran. Since the heat to power ratio of a common SOFC system is 2:1, an efficient heat recovery system has been considered to supply the heat required by the steam producer and recuperative heat exchangers. All the main components in the comprehensive system were modeled and then simulated. Results showed high total energy efficiency along with minimum heat loss are feasible in the proposed cycle. Moreover, desirable methane and hydrogen conversion ratios have been attained when utilizing this system for commercial power generation purposes. Lastly, a cathode recycling effect on the MSR combustor operation has been indicated.

1. Introduction

The hydrogen economy focuses on the production of energy from hydrogen, which is the most abundant element on earth, with minimum environmental impact. One of the technologies that fit into the concept of the hydrogen economy is the fuel cell. This work focuses on solid oxide fuel cells (SOFC)

*Corresponding Author's Fax: 00982156276632
E-mail address: allahyari@irost.ir

doi:10.22104/ijhfc.2017.2392.1151

and their synergism with conventional devices of energy production [1-3].

Methane is the main component of natural gas and a side product of many petrochemical processes and gasification. Reforming of the methane molecule has become one of the most extensively studied reforming reactions because of its common appearance and relative simplicity. There are two main types of methane reforming, referred to as wet and dry reforming [4-7].

For the conditions of SOFC operation, wet reforming is generally considered to be the most practical type of reforming [8]. Most studies on methane reforming in SOFCs are therefore investigating methane steam reforming.

Design configurations of natural-gas and hydrogen-fueled SOFC-based micro-CHP systems for residential applications have been presented and analyzed by Braun et al. [9]. Results for two different hydrogen system configurations and four different natural gas system configurations have been presented. System electric efficiencies of 40% HHV (45% LHV) were described.

Several SOFC systems with MSR have already been demonstrated. Powell et al. [10] operated a SOFC with MSR from 1.65 to 2.15 kW with 57% to 53% DC electrical net efficiency. Powell et al. state that the net efficiency could be further improved to over 60% with the use of properly sized blowers. In the framework of the RealDemo–project, the Technical Research Centre of Finland (VTT) operated a 10 kW cross-flow SOFC with AOR at an AC net electrical efficiency of 54% [11, 12]. All efficiencies in this section are based on the lower heating value (LHV).

A mathematical model for a planar SOFC was constructed by Yakabe et al. [13] to calculate concentration of the chemical species, the temperature distribution, the potential distribution and the current density using a single-unit model. External steam reforming, water-shift reaction and diffusion of gases in the porous electrodes considered in the model. The results demonstrated that steam reforming would generate high internal stress in an electrolyte.

A sufficient amount of steam is necessary in the reformer to fulfill the reforming reaction requirements. Previous studies on methane reforming in SOFCs have shown that a steam to carbon ratio higher than 2 guarantees that carbon formation does not occur in the SOFC [14]. However, a very high steam to carbon ratio can prove to be an inefficient choice, as it would dilute the hydrogen in the fuel channel, lowering the electrical efficiency of the cell. Therefore, the steam to carbon ratio is usually kept below 3.5 [15].

Al-Sulaiman et al. [16] have conducted an energy analysis of a trigeneration plant based on a SOFC and organic Rankine cycle. They found that the highest net power output that can be provided by the plant considered was 540 kW and, the highest SOFC power was 520 kW. The study also showed that the maximum efficiency of the electricity production was 46%.

Meshcheryakov et al. [17] presented a thermodynamic analysis of a solid oxide fuel cell power system using conditions of thermodynamic equilibrium in a pre-reformer of natural gas to synthesis gas and a solid oxide fuel cell battery. It was shown that a thermally coupled steam reformer of natural gas provides a significantly higher efficiency of conversion of fuel energy to electric energy than other types of reformers. Energy efficiency of system has been calculated at about 50% for 0.4 degree of recirculation of the exhaust anode gas at 0.6 degree of fuel consumption.

Becker et al. [18] focused on the design and performance estimation of a methane-fueled, 1 MW SOFC combined heat, hydrogen, and power system. Two methods of hydrogen purification and recovery from the SOFC have been analyzed in their research. The SOFC electrical efficiency at rated power was estimated at 48.8%.

The methodology, operation, and simulation of a large-scale 1 MW SOFC–CHP power plant as well as the system configuration and major component models were discussed by Colson and Nehrir [19]. End-use electricity and hot water consumption profiles were developed for residential customers.

Total energy efficiency of the presented system has been indicated about 50%.

A conceptual design of a 5 MW natural gas fueled solid oxide fuel cell system for distributed power generation was developed at the US Department of Energy [20] based on knowledge of state-of-the-art SOFC stack technology. System efficiency and stack voltage achieved around 57% and 0.83 V, respectively.

A natural gas fueled SOFC power system was modeled by Chick et al. [21]. In their system, the reformer is referred to as adiabatic because no extra heat needs to be supplied to support the reaction. The single-pass fuel utilization was about 55%, but because of the recycle arrangement the overall fuel utilization was about 93%. They proposed that at an operational pressure of 8 bar and 0.825 volts per cell, this pressurization increases the power density of the stack by about 70%.

Despite several years of investigation, the steam reforming of methane in SOFCs is still poorly understood. This is reflected in the large number of heat loss expressions that are derived from the MSR process. This makes the modeling of methane reforming and its influence on the cell performance very challenging. Because of these difficulties, only a limited number of modeling studies have developed their results to comprehensive cycles.

Additionally, natural gas reforming does not require cleaning before being used within the SOFC, whereas several systems have to be employed to clean up the syngas generated by other resources (e.g. biomass gasification).

Several disadvantages/challenges encountered in the construction and exploitation of SOFCs include insufficient thermal resistance, complexity arising from the need for reforming of hydrocarbon fuels, insufficient overall energy efficiency of SOFC stacks, and insufficient utilization of the fuel in the anode. Solutions to those technical barriers must be found in order to achieve technological maturity and cost reduction of SOFC technology. Hence, a hydrogen production based on external steam reforming of natural gas and heat recovery opportunities to increase total energy efficiency is explored/ studied/ researched in this paper.

Researchers have tried to simplify the thermal efficiency problem by separating out all other influences. In this study, a new method for analyzing an SOFC cycle fueled by external natural gas reforming has been developed. Furthermore, some of the discussed issues are addressed. The electrochemistry and water gas shift reaction are additional complications that have to be considered. With this approach the authors tried to:

• Study the influence of fuel cell geometry input data, such as cell area and cell resistance, on the cell voltage and fuel consumption;

• Evaluate the use of an integrated model for the fitting of heat recovery data obtained in operational SOFCs;

• Investigate possible Methane Steam Reforming mechanisms on SOFC anodes;

• Study the influence of steam/fuel ratio on the MSR output and SOFC cycle efficiency.

Finally, since fuel accessibility is one of the most challenging issues for fuel cell power plants; the great potential of natural gas in Iran makes this cycle much more attractive.

2. System configuration

A comprehensive system configuration has to be investigated to determine the most efficient and suitable system. A system conceptual diagram of the baseline configuration for the proposed case is shown in Fig. 1. A MSR based system was chosen because it gives a high molar fraction of hydrogen and carbon monoxide. In addition to this case, an improved system configuration with bypass of anode and cathode gases is being investigated.

The NG enters the system at node 1 and is then preheated and mixed with stream at recuperator No .2 and the MSR, respectively. The mixture entering the MSR has a temperature of about 400°C, there long chained hydrocarbons and some of the methane are converted primarily into hydrogen and carbon monoxide.

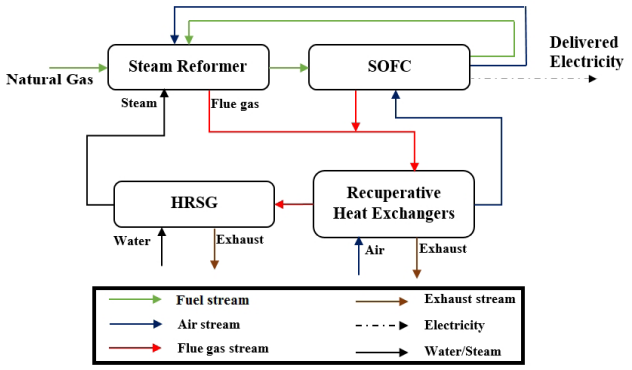

Fig. 1. Conceptual schematic of the proposed cycle.

This reformed gas enters the anode side of the SOFC stack by stream No. 3, where the residual methane is initially converted and the hydrogen electrooxidated. The SOFC is operated at 950°C. Simultaneously, air is blown into the cathode side from stream No. 44. It is filtered, compressed and then preheated through recuperators Nos. 42, 43 and 44 and blower No. 41 before entering the SOFC. Meanwhile, a given amount is recycled at stream No. 5 and is blown into the combustor to control the flame temperature at stream No. 7.

Electricity is generated and transmitted to an inverter which converts it from a DC to an AC current. This current then supplies pumps and blowers in the system. The residual electricity is the net AC power. In addition, the SOFC also produces an exhaust gas. The cathode and anode exhaust gasses are now mixed and combusted in a catalytic burner together. If the addition of air and NG is necessary, both will be injected to control the catalytic combustion temperature and to satisfy the thermal demand. The hot product gas flows into the MSR and to the heat exchange with the reformer to deliver the heat required by the reforming process. Afterward, this hot gas heat exchanges further with the NG, the water feed, and the cathode air before finally leading to the exhaust stack.

The steam producer system consists of an economizer, an evaporator, and a super heater to generate the required steam for the MSR unit. Moreover, surplus produced steam is consumed as a steam network in downstream processes.

The main elements and streams of the simulated system have been demonstrated in Fig. 2.

3. System simulation

The system and sub-systems are modeled and then simulated in Cycle Tempo software since it is capable of solving large systems of non-linear equation and has built-in thermal properties. The sub-systems are made with modules and connected according to the system design. The method of system simulation is based on stationary conditions along with conversion of streams analysis.

3.1.Assumptions

To facilitate low computational time and numerical stability in Cycle Tempo, the system has been modeled under different assumptions and simplifications. These assumptions are listed below:

• The chemical reactions of the MSR are assumed to reach chemical equilibrium;

• Carbon formation in the system is not modeled since it is assumed avoided by using high steam-to-carbon ratios;

• All components except reformer, SOFC, and combustor have been modeled as being adiabatic;

• Pressure losses due to piping are neglected since the components are closely placed. However, component pressure losses are approximated based on values found in the literature;

• The system is evaluated at steady state, neglecting transient effects, and thereby reflecting nominal use;

• The power electronic DC/AC inverter is approximated as a default with an electrical efficiency of 96%;

• The SOFC is assumed as being thermodynamically lumped. So, all streams are distributed uniformly in the cells.

The steam-to-carbon ratios have been chosen to avoid carbon formation and are based on empirical knowledge of previous studies [17]. It, therefore, seems acceptable to neglect any modeling of carbon

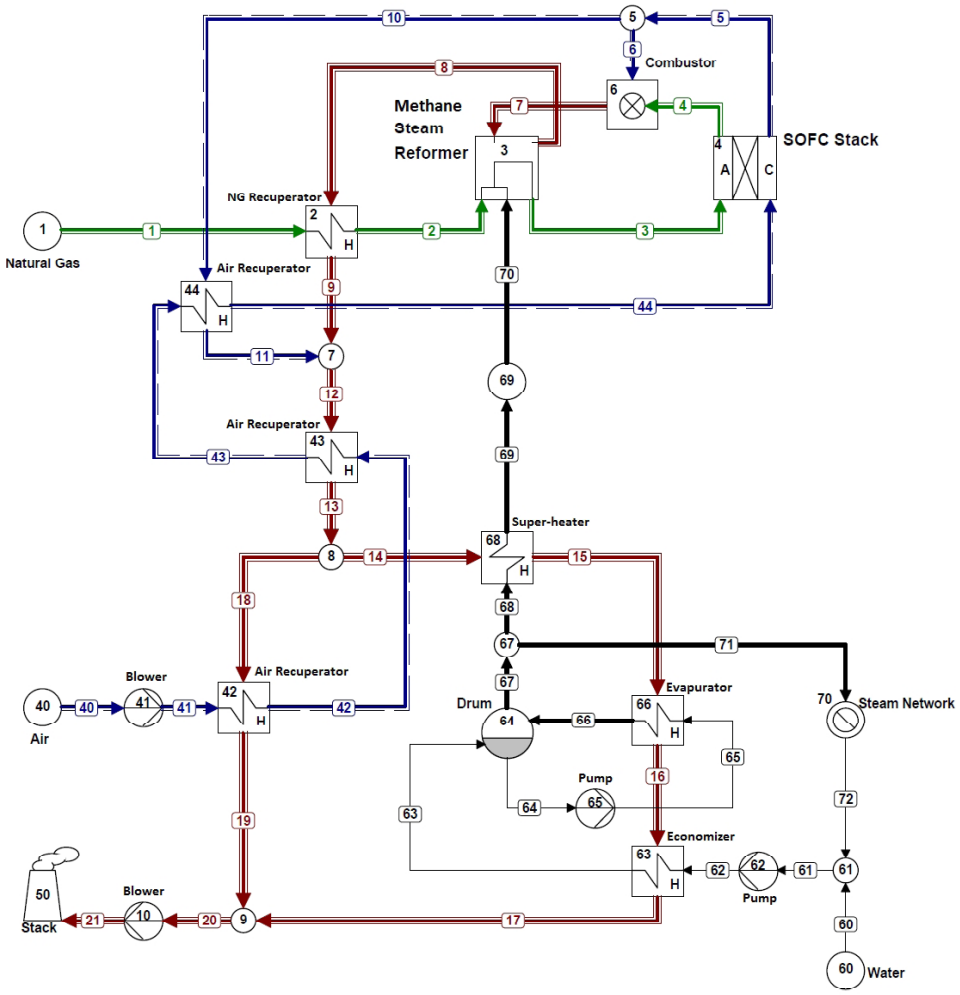

Fig. 2. Sketch of the simulated external reforming SOFC.

formation. Any modeling of carbon formation would further require experimental knowledge about the real reactor design.

The composition of the standard natural gas used in the proposed cycle is shown in Table 1.

Table 1. Composition of the natural gas [22].

Component	Mole (%)
CH_4	81.29
C_2H_6	2.87
C_3H_8	0.38
C_4H_{10}	0.15
C_5H_{12}	0.04
C_6H_{14}	0.05
CO_2	0.89
N_2	14.32
O_2	0.01
LHV (kJ/kg)	37998.9

3.2. System Parameters

The primary parameters of the system design are the thermal, electrical and total efficiencies. These parameters are used to compare system feasibility. They are stated as follows:

$$\eta_{el} = \frac{P\eta_{inverter} - W_{parasitic}}{LHV_{NG}.\dot{m}_{NG}} \quad (1)$$

$$\eta_{th} = \frac{P_{th}}{LHV_{NG}.\dot{m}_{NG}} \quad (2)$$

$$\eta_{tot} = \eta_{el} + \eta_{th} \quad (3)$$

Where, $W_{parasitic}$ is the parasitic work loss due to compressors, pumps or blowers (W).

Among other factors, system efficiency depends on the amount of methane pre-reforming since the more internal reforming the better cooling of the SOFC and thus less air is needed.

The Degree of Steam Reforming (DOSR) is therefore stated as follows to monitor this parameter:

$$DOSR = 1 - \frac{\dot{n}_{CH_4,\,out}}{\dot{n}_{CH_4,\,in}} \tag{4}$$

Where and is the molar flow out and in to the steam reformer,respectively, since the highest proportion of natural gas is methane. The system efficiency further depends on the amount of Cathode Gas Recycled (CGR), this is stated as follows:

$$CGR = \frac{\dot{m}_{recycled}}{\dot{m}_{SOFC,\,out}} \tag{5}$$

3.3.Natural gas steam reforming

Hydrogen can be produced from steam forming out of natural gas. It takes place in the presence of a steam medium. Hydrocarbon steam reforming turns hydrocarbons into their compounds. It is the most widely used process in the industrial manufacture of hydrogen [23]. The overall MSR reaction of methane and higher hydrocarbons is given by:

$$CH_4 + H_2O \rightarrow 3H_2 + CO,\ \Delta h = 206\left(kJ/mol\right) \tag{6}$$

The reactions are endothermic and are as such energy intensive and require an external heat source. Hence, the stream is typically preheated to 450 to 650 (°C) before entering the reactor. The reactions then take place in a nickel-based catalyst bed at temperatures of about 750 to 900 (°C), as the highest methane conversion is possible there.

Further, it is apparent from previous studies that a high molar fraction of hydrogen to carbon monoxide is possible with MSR. This gives a higher SOFC efficiency than with other reforming technologies [24], and due to the high hydrogen fraction produced it is called the most economical route to produce hydrogen [25]. If necessary, the MSR process can operates at high pressures.

Since the reactions require a large amount of heat the reactor is often built as a heat exchanger as shown in Fig. 3.

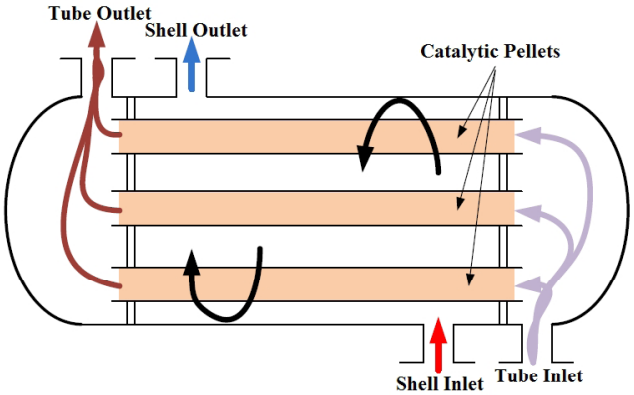

Fig. 3. Schematic natural gas steam reformer design.

At the shell inlet, the hot flue gas from the burner is fed to heat up the tubes; the flue gas is then cooled down and escapes from the reformer at the tube outlet. Catalytic pellets, normally Ni-based, are placed inside the tubes. The desulphurised NG mixed with steam is fed into the tube inlet, and the product gasses come out at the tube outlet.

For the adiabatic steam reforming reactor the first law of thermodynamics gives:

$$\sum_i \dot{m}_{i,\,MSR} h_{i,\,MSR} = \sum_e \dot{m}_{e,\,MSR} h_{e,\,MSR} \tag{7}$$

The mass flow rate of the reactants is calculated in terms of their molar flow rates and their molecular weights. On a mole basis, the terms of the above equation can be rewritten as follows:

$$\sum_i \dot{m}_{i,\,MSR} h_{i,M\,SR} = \sum_i \dot{N}_{i,\,MSR} \overline{h}_{i,\,MSR} \tag{8}$$

$$\sum_e \dot{m}_{e,\,MSR} h_{e,\,MSR} = \sum_e \dot{N}_{e,\,MSR} \overline{h}_{e,\,MSR} \tag{9}$$

Where the subscript i refers to the reactants of the steam reforming reactor and those are H_2O, CH_4, CO and CO_2, and e refers to the products of the steam reforming reactor and those are H_2, CO, and CO_2.

The reaction is often carried out with excess steam-

to-carbon ratios above 2.5 to avoid carbon deposition (coke) on the catalyst surface [26].

In addition to the MSR, the Water Gas Shift (WGS) reaction is:

$$CO + H_2O \rightleftarrows CO_2 + H_2,\ \Delta h = -41\left(kJ/mol\right) \quad (10)$$

The outlet composition contains hydrogen, water, carbon monoxide, carbon dioxide and unconverted methane. WGS reactions are thermodynamically favored at low temperature and pressure [27]. However, due to slow reaction kinetics, a catalyst is normally used.

Normally, the focus is on utilizing the WGS reaction to lower the amount of carbon monoxide and increase the amount of hydrogen in the synthesis gas. In theory, this is not necessary in the case of an SOFC since carbon monoxide can be used as fuel. In practice, CO is not favorable as fuel which is described later.

A sketch of the input and outputs of the SR model along with the main compositions of fluids are shown in Fig. 4.

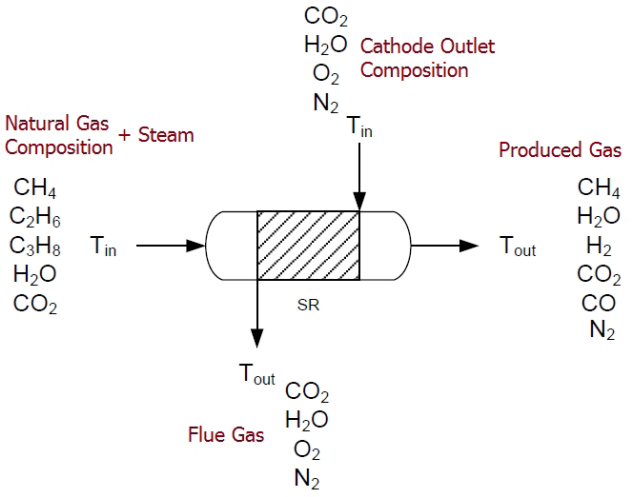

Fig. 4. Sketch of the steam reformer.

3.4.Combustor

The catalytic combustion burns the exhaust gas from the SOFC, which is then bypassed into the combustor to supply enough heat for steam reforming. The advantage of employing a catalytic burner as opposed to a pyrolytic burner is a lower operational temperature. Thus, the material demand for constructing the components decreases. The overall reaction mechanism can be described as follows:

$$CH_4 + 2O_2 \rightarrow CO_2 + 2H_2O \quad (11)$$

$$H_2 + \frac{1}{2}O_2 \rightarrow H_2O \quad (12)$$

$$CO + \frac{1}{2}O_2 \rightarrow CO_2 \quad (13)$$

Based on the considered fuel the air stoichiometry can be stated as follows:

$$\dot{n}_{O_2,stoich} = \frac{1}{2}\dot{n}_{CH_4} + 2\dot{n}_{H_2} + 2\dot{n}_{CO} \quad (14)$$

$$\lambda_{air} = \frac{\dot{n}_{O_2}}{\dot{n}_{O_2,stoich}} \quad (15)$$

3.5.Solid oxide fuel cell

Two common SOFC designs exist, tubular and planar. One advantage of tubular designs is that high-temperature gas tight seals are eliminated, but the planar design that resembles the design of PEM FCs is easier to fabricate [1]. Therefore, the planar type has been considered in this study.

The SOFC operates at temperatures around 700-1000 (°C) and uses a special ceramic material as the electrolyte. The reactions taking place at the electrodes with hydrogen and air (oxygen) as reactants can be seen in Equations 16 and 17 [2].

Anode:

$$2H_2 + 2O^{2-} \rightarrow 2H_2O + 4e^- \quad (16)$$

Cathode:

$$O_2 + 4e^- \rightarrow 2O^{2-} \quad (17)$$

In contrast to most other FCs, the water is produced at the anode in SOFCs. Where CO acts as a poison in most FCs, it can theoretically act as a fuel in an SOFC according to the anode reaction shown in Equation 18.

Anode:

$$2CO + 2O^{2-} \rightarrow 2CO_2 + 4e^- \quad (18)$$

The different components of the SOFC are depicted in Fig. 5. The anode, cathode, and electrolyte are normally based on ceramic materials.

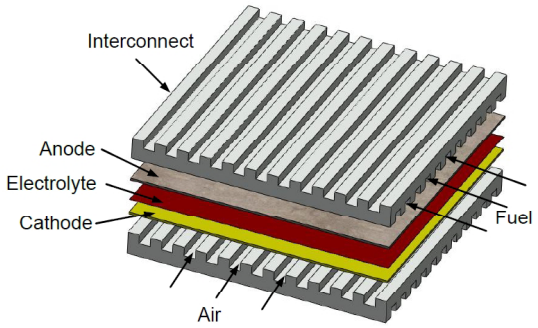

Fig. 5. Overview of a single planar SOFC.

In Fig. 6 the energy balance of an SOFC is demonstrated.

The reactants deliver the total enthalpy to the system, $\Sigma n_i H_i$, and the total enthalpy leaving the system is $\Sigma n_j H_j$. Also, W_{trev} is the reversible work transferred from the SOFC to the environment and Q_{rev} is the heat extracted from the SOFC to the environment.

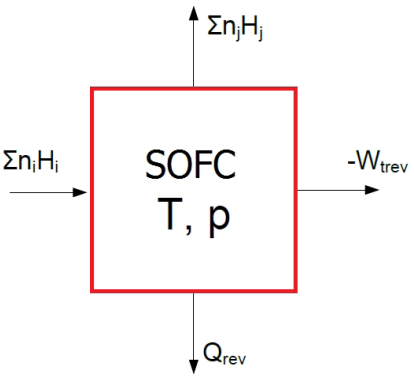

Fig. 6. The energy balance and system boundary of a reversible SOFC.

In Fig. 7 the different transport processes in an SOFC with hydrogen as a fuel can be seen.

As shown in Fig. 7, the product water is mixed with the anode gas and its concentration increases with increasing fuel utilization U_f which is defined by:

$$U_f = 1 - \frac{\dot{m}_{F,\,anode,\,out}}{\dot{m}_{F,\,in}} \quad (19)$$

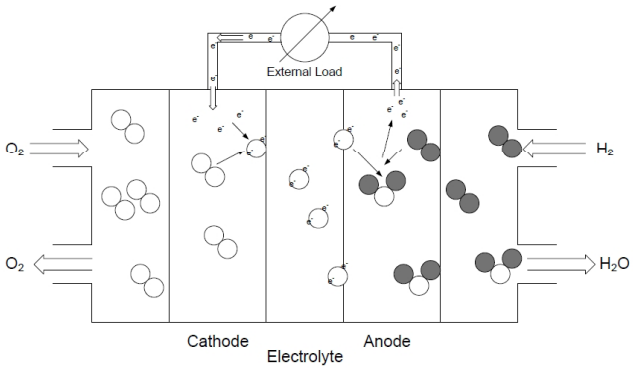

Fig. 7. Schematic of the transport processes in an SOFC with hydrogen as fuel.

In addition, the molar flow of electrons is two times the molar flow of hydrogen, thus:

$$\dot{n}_{el} = 2\dot{n}_{H_2} \quad (20)$$

The electric current I is a linear function of the molar flow of electrons, shown in Equation 21 [28].

$$I = \dot{n}_{el}.(-e).N_A = -\dot{n}_{el}.F = -2\dot{n}_{H_2}.F \quad (21)$$

The Faraday constant is (C/mol).

The reversible power can be written as a product of the reversible voltage $V_{FC,rev}$ and the current I as well as the product of the Gibbs free enthalpy and the molar flow of the fuel:

$$P_{FC,\,rev} = V_{FC,\,rev}.I = \dot{n}_{H_2}.\dot{w}_{FC,\,rev} = \dot{n}_{H_2}.\Delta^r G \quad (22)$$

The reversible voltage $V_{FC,rev}$ results from Equations 22 and 23.

$$V_{FC,rev} = \frac{-\dot{n}_{H_2}.\Delta^r G}{\dot{n}_{el}.F} \quad (23)$$

The above equations are for hydrogen as fuel, but the reversible voltage for any fuel can be written as:

$$V_{FC,rev} = \frac{-\Delta^r G}{n_{el}.F} \quad (24)$$

The reversible voltages for CO, CH_4, and H_2 as fuels have been calculated and the reactions used are presented in Equations 11 to 13.

By assuming ideal gasses the Nernst potential or Nernst voltage V_N can be expressed as:

$$V_N = \frac{-\Delta^r G(T)}{n_{el}.F} - \frac{R_u.T.Ln(K)}{n_{el}.F} \quad (25)$$

The equilibrium constant is:

$$K_{eq} = \prod_j \left(\frac{p_j}{p_0} \right)^{v_j} \quad (26)$$

Where, v_j is the fuel-related quantity of the component j in the oxidation reaction equation [28].

As already described, mixing of the gasses in the SOFC makes the reversible operation impossible. These influences and the followed voltage reduction can be calculated by considering the fuel utilization connected with a change in the partial pressures of the components within the system [28]. An example to illustrate this is the oxidation of hydrogen (Equation 12). The partial pressure of each component is:

$$p_i = y_i.p \quad (27)$$

Equation 20 can be expressed as:

$$U_f = 1 - \frac{y_{F,\,in}.\dot{n}_{anode,\,in} - y_{F,out}.\dot{n}_{anode,\,out}}{y_{F,\,in}.\dot{n}_{anode,\,in}} \quad (28)$$

The local Nernst voltage as a function of the fuel utilization ($N_N(U_f)$) depends on the local gas concentration. In the example of hydrogen as the fuel, the molar flow on the anode side is constant:

$$\dot{n}_{anode,\,in} = \dot{n}_{anode,\,out} = \dot{n}^* \quad (29)$$

and Equation 19 yields:

$$U_{f,H_2} = 1 - \frac{y_{H_2,out}}{y_{H_2,in}} \quad (30)$$

The number of moles of utilized oxygen is equal to twice the moles of hydrogen used:

$$\dot{n}_{O_2,U} = \frac{1}{2}\dot{n}_{H_2,U} \quad (31)$$

Normally, SOFC systems are run with air instead of oxygen and with excess air (λ>1). The incoming air at the cathode is defined as [28]:

$$\dot{n}_{cathode,\,in} = \frac{1}{2}.\lambda.\frac{\dot{n}^*}{0.21} \quad (32)$$

And the outlet flow:

$$\dot{n}_{cathode,out} = \frac{1}{2}.\lambda.\frac{\dot{n}^*}{0.21} - \frac{1}{2}\dot{n}_{H_2,U} \quad (33)$$

The related oxygen flow at the inlet and outlet is, respectively:

$$\dot{n}_{O_2,\,in} = \frac{1}{2}.\lambda.\dot{n}^* \quad (34)$$

$$\dot{n}_{O_2,\,out} = \frac{1}{2}.\left(\lambda.\dot{n}^* - \dot{n}_{H_2,U}\right) \quad (35)$$

Equations 33 and 35 can now be expressed as a function of U_f:

$$\dot{n}_{cathode,out} = \frac{1}{2}.\dot{n}^*.\left(\frac{\lambda}{0.21} - \frac{\dot{n}_{H_2,U}}{\dot{n}^*}\right) = \frac{1}{2}.\dot{n}^*.\left(\frac{\lambda}{0.21} - U_{f,H_2}\right) \quad (36)$$

$$\dot{n}_{O_2} = \frac{1}{2}.\dot{n}^*.\left(\lambda - \frac{H\ U}{}\right) = \frac{1}{2}.\dot{n}^*.\left(\lambda - U_{f\ H_2}\right) \quad (37)$$

Now the molar concentrations xi can be written as a function of U_f:

$$y_{H_2,out} = 1 - U_{f,H_2} \quad (38)$$

$$y_{H_2O,out} = U_{f,H_2} \quad (39)$$

$$y_{O_2,out} = \frac{\lambda - U_{f,H_2}}{\frac{\lambda}{0.21} - U_{f,H_2}} = \frac{\dot{n}_{O_2,\,out}}{\dot{n}_{Cathode,out}} \quad (40)$$

Finally, the Nernst voltage (E_N) can be expressed as a function of the fuel utilization:

$$E_N = \frac{-1}{n_{el}.F}\left[-\Delta^r G(T) + T.R_u Ln\left(\frac{U_{f,H_2}\left(\frac{\lambda}{0.21} - U_{f,H_2}\right)^{1/2}}{\left(1 - U_{f,H_2}\left[\left(\lambda - U_{f,H_2}\right).p\right]^{1/2}\right)}\right)\right] \quad (41)$$

The current is proportional to the fuel utilization in the following manner [29]:

$$U_f = \frac{I}{n_{el}.\dot{n}_{F,in}.F} \quad (42)$$

To drive the chemical reactions at the anode and cathode some voltage is lost to overcome the

activation energy barrier of the exothermic reaction. The activation overvoltage is proportional to current density and can be determined by the Butler-Volmer equation:

$$i = i_0 \left[exp\left(\alpha \frac{n_e F}{R_u T_{SOFC}} V_{act} \right) - exp\left(-(1-\alpha) \frac{n_e F}{R_u T_{SOFC}} V_{act} \right) \right] \quad (43)$$

Where n_e is the number of electrons transferred per hydrogen molecule reacted. The exchange current density gives the equilibrium rate at which reactants and product species are exchanged equally, i.e. zero current density and thus in the absence of an activation overvoltage [30]. The activation overvoltage is solved for both the anode and cathode, by substituting their respective exchange current density that is calculated as follows [31]:

$$i_{0,\,anode} = \gamma_{anode} \frac{y_{H_2}^{anode} P_{anode}}{P^0} \left(\frac{y_{H_2O}^{anode} P_{anode}}{P^0} \right)^{-0.5} \exp\left(\frac{-E_{act,\,anode}}{R_u T_{SOFC}} \right) \quad (44)$$

$$i_{0,\,cathode} = \gamma \left(\frac{y_{O_2}^{cathode} P_{cathode}}{P^0} \right)^{0.25} \exp\left(\frac{-E_{act,\,cathode}}{R_u T_{SOFC}} \right) \quad (45)$$

The total activation voltage is then the sum of each individual activation overvoltage:

$$V_{act} = V_{act,\,anode} + V_{act,\,cathode} \quad (46)$$

The anode overvoltage is typically very low compared to the cathode. It should further be noted that activation overvoltages are rather low due to the elevated temperatures.

The concentration overvoltage describes the incremental voltage loss due to reactant depletion in the catalyst layer. Thus, it can be calculated as the difference between the Nernst potential at the catalyst layer and the bulk flow at both anode and cathode. Based on the limiting current the total concentration overvoltage can be expressed as follows:

$$V_{conc} = \frac{R_u T_{SOFC}}{2F} Ln\left[\left(\frac{i_{l,H_2}}{i - i_{l,H_2}} \right) \left(\frac{i_{l,O_2}}{i - i_{l,O_2}} \right)^{0.5} \right] \quad (47)$$

The limiting current density is defined as the case where the reactant concentration in the catalyst layer drops to zero at steady-state, i.e. representing the maximum possible current density. This can be determined using the following equation:

$$i_{l,\,i} = \frac{e_n F D^{eff} C_{i,0}}{\nu_i \delta} \quad (48)$$

Where, $C_{i,0}$ is the concentration of species i of the bulk fluid and vi is the stoichiometry coefficient of species i in the reaction. The effective diffusivity depends on the porous structure of the electrode and can be expressed as follows at high temperatures [30]:

$$D^{eff} = D \frac{\varepsilon}{\tau} \quad (49)$$

Where, τ is the tortuosity, i.e. impedance to diffusion caused by a tortuous or convoluted path. If ideal gas behavior is assumed, the concentration of species i can be calculated with:

$$C_{i,\,0} = \frac{y_i P}{R_u T_{SOFC}} \quad (50)$$

Where P is pressure (Pa).

The ohmic voltage loss can be described by Ohm's law of conductivity. The total resistance is given as the sum of the resistance through the electrodes, electrolytes and the interconnectors:

$$V_{ohm} = iR = i \sum r_j \quad (51)$$

Usually the electrolyte resistance dominates [28].

The governing equation for the irreversible cell voltage can thus be calculated as the OCV minus the sum of the overvoltages:

$$V_{cell} = V_{OCV} - V_{act} - V_{conc} - V_{ohm} \quad (52)$$

The stack voltage, current, and power are given by the following equations:

$$V = n_{cell} V_{cell} \quad (53)$$

$$I = iA_{fc} \quad (54)$$

$$P = VI \quad (55)$$

The hydrogen consumption can be related to the current drawn by Equation (22) and multiplied by the

number of cells in the stack. Input parameters to the SOFC unit are shown in Table 2 [32, 33].

Table 2. Input parameters of SOFC and MSR

Parameter	Value (unit)
Fuel utilization factor	0.85
SOFC Reaction pressure	1 (bar)
SOFC Reaction temperature	950 (°C)
Stack area	700 (m^2)
Cell resistance	7.5×10^{-5} (Ω)
DC/AC conversion efficiency	0.96
Anode and cathode inlet temperature	850 (°C)
Steam reformer reaction pressure	1 (bar)
Steam reformer reaction temperature	800 (°C)

Additionally, rotating equipment characteristics have been indicated in indicated in Table 3.

Table 3. Rotating equipment characteristics

Apparatus name	Isentropic Efficiency (%)	Mechanical efficiency (%)
Flue gas compressor	80	100
Air compressor	75	100
Feed water pump	85	100
Circulating pump	75	100

Furthermore, input data of the fuel, air and water inlets are presented in Table 4.

Table 4. Fuel, air and water input data

Parameter	Value (unit)
Fuel inlet temperature	15 (°C)
Fuel inlet pressure	1.18 (bar)
Feed water inlet temperature	20 (°C)
Feed water inlet pressure	1.2 (bar)
Air inlet temperature	15 (°C)
Air inlet pressure	1.013 (bar)

4.Results and discussions

The calculations have been performed for the proposed system. Based on these calculations, the efficiency and performance of the cycle have been determined. The main results of the system are presented in Table 5.

The gross efficiency is calculated by dividing the total delivered gross electrical power by the total absorbed heat power. Since the presented combined cycle is a CHP system, the total cycle efficiency, which is about 53%, is significant for single SOFC cycles. The net efficiency is calculated by dividing the total delivered net electrical power by the total absorbed heat power.

The residual heat (from the sink No. 70 in Fig.2) can be used to generate steam in the boilers of a bottoming steam cycle or endothermic process. The total amount of steam transferred to this network is 0.059 kg s^{-1}.

In Table 6, the compositions of the resulting fluids (pipes 3 and 4) for the presented system are given.

Table 5. Performance and efficiency of the considered cycle

Performance or efficiency term	Value
Absorbed power (kW)	1884.79
Delivered gross power	
ER-SOFC (kW)	1000.00
Auxiliary power consumption	
Flue gas compressor (kW)	63.79
Air compressor (kW)	96.72
Feed water pump (kW)	0.37
Circulation pump (kW)	0.80
Net power (kW)	838.32
Delivered heat (kW)	159.02
Total delivered (kW)	997.35
Efficiencies	
Gross (%)	53.05
Net (%)	44.48
Heat (%)	8.44
Total (%)	52.92

The residual heat (from the sink No. 70 in Fig.2) can be used to generate steam in the boilers of a bottoming steam cycle or endothermic process. The total amount of steam transferred to this network is 0.059 kg s^{-1}.

In Table 6, the compositions of the resulting fluids (pipes 3 and 4) for the presented system are given.

Furthermore, according to Equation 4 and Table 6, the DOSR gives a value of 99.96%, which shows

a high methane conversion rate in the reforming process.

Table 6. Composition in mole% of the fluids in fuel pipes of the system

Component (unit)	Stream 3	Stream 4
Mass flow (kg s^{-1})	0.193	0.32
Temperature (°C)	850	1010
Pressure (bar)	1.15	1.10
H_2	51.51	7.16
CH_4	0.03	0.03
CO	9.50	1.90
CO_2	6.11	13.70
N_2	2.48	2.48
H_2O	30.37	74.73

A comparison between the presented study and some previous related experiences is demonstrated in Table 7. Power production capacity and system efficiency are two benchmarking factors. According to these values, the achieved results of the proposed cycle are satisfactory comparable with indicated references.
Resulting amounts for some important pipes of the proposed plant illustrated in Fig. 2, are indicated in Table 8.

Table 7. Comparison of energy efficiency with four related references

Reference	Capacity	Total efficiency	Electrical efficiency
Ref. No. 16	520 kW	N/A*	46.0%
Ref. No. 18	1 MW	N/A	48.8%
Ref. No. 19	1 MW	50.0%	N/A
Ref. No. 20	5 MW	57.0%	N/A
Current study	1 MW	52.9%	53.0%

*N/A: Not Available

Based on Table 8 and Equation 5, the CGR value calculated 21.94% which is the recycled amount of cathode outlet consumed in the combustor. Also, the compositions of each medium are demonstrated in Table 9. It should be noted that GasMix 1 and 8 are natural gas and water, respectively.
The calculated heating values of all presented fluid compositions are indicated in Table 10.

Due to obtained results of Tables 9 and 10, the high hydrogen production rate of MSR caused the significant heating value of GasMix 2 (more than 51%). However, MSR of natural gas is the most conventional and commercial method of hydrogen production. As mentioned before, some heat exchangers have been considered in the comprehensive system design to minimize the heat loss rate of the proposed cycle. Therefore, Table 11 shows the outputs of the simulation of heat exchanger characteristics.
The effect of the steam/fuel ratio on the total energy efficiency of the proposed cycle is presented in Fig.8. As it is shown, a steep reduction of efficiency occurs by increasing the rate of steam/fuel in the MSR.

5. Conclusion

In this study, a novel method to develop a SOFC system along with the MSR of natural gas was proposed to achieve high delivered power and total energy efficiency. Therefore, the following conclusions are based on the results of this study.

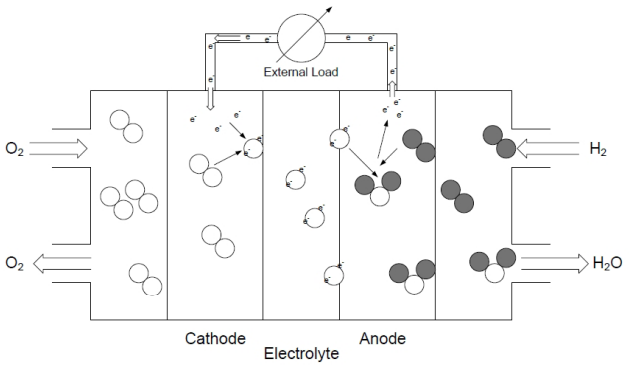

Fig. 8. Effect of steam to fuel ratio on total cycle efficiency.

• Maximum plant energy efficiency (about 53%) has been gained at a steam/fuel ratio of 2.887 and 85% utilization factor.
• Around 51.5% of the hydrogen production rate is obtained by steam reforming of natural gas, where it is used as a fuel production mechanism.
• The heat energy efficiency of the proposed system is about 8%, which is consumed in a steam network.
• The degree of steam reforming and cathode gas

Table 8. Results of selected pipes

Pipe No.	Medium	Mass flow (kg s^{-1})	Pressure (bar)	Temperature (°C)	Enthalpy (kJ kg^{-1} k^{-1})
2	GasMix 1	0.050	1.16	400.00	-2724.12
3	GasMix 2	0.193	1.15	850.00	-6401.67
4	GasMix 3	0.320	1.10	1010.00	-9487.84
5	GasMix 4	4.498	1.10	1010.00	994.29
6	GasMix 4	0.987	1.10	1010.00	994.29
7	GasMix 5	1.308	1.09	1200.00	-1574.27
8	GasMix 5	1.308	1.04	814.31	-2123.76
12	GasMix 6	4.418	1.02	761.94	-83.93
13	GasMix 6	4.418	1.00	495.64	-398.85
14	GasMix 6	1.511	1.00	495.64	-398.85
21	GasMix 6	4.818	1.013	105.85	-827.49
42	GasMix 7	4.625	1.18	350.00	246.31
43	GasMix 7	4.625	1.16	648.72	574.35
63	Water	0.203	10.20	160.78	679.20
64	Water	2.115	10.20	180.75	766.49
65	Water	2.115	11.70	180.78	766.72
66	Water	2.115	10.20	180.75	967.63
67	Water	0.203	10.20	180.75	2777.87
70	GasMix 8	0.143	9.70	400	-12706.65
71	Water	0.059	10.20	180.75	2777.87

Table 9. Composition in mole% of all fluids

Composition No.	2	3	4	5	6	7
CH_4	0.0003	0.0003	-	0.5631	0.7269	0.7729
N_2	0.0248	0.0248	0.7926	0.1168	0.1671	0.2075
O_2	-	-	0.1873	0.0492	0.0143	0.0003
CO_2	0.0611	0.1370	0.0003	0.2642	0.0831	0.0101
H_2O	0.3037	0.7473	0.0104	0.0066	0.0086	0.0092
Ar	-	-	0.0094	-	-	-
H_2	0.5151	0.0716	-	-	-	-
CO	0.0950	0.0190	-	-	-	-

Table 10. Heating values of all compositions

Composition No.	LHV (kJ/kg)	HHV (kJ/kg)	LHV without water (kJ/kg)	HHV without water (kJ/kg)
1	37999.18	42107.15	37999.18	42107.15
2	12078.48	13884.84	21407.12	24608.59
3	1097.93	1249.96	3039.71	3522.09
4	0.00	0.00	0.00	0.00
5	0.03	0.03	0.04	0.04
6	0.01	0.01	0.01	0.01
7	0.00	0.00	0.00	0.00
8	0.00	0.00	0.00	0.00

recycled has been calculated at 99.96% and 21.94%, respectively.

• The significant natural gas resources of Iran might provide a great opportunity for generating green energy by this efficient SOFC cycle.

Nomenclature

A_{fc}	Effective cross sectional area (m^2)
C	Concentration (mol m^{-3})
D	Diffusion coefficient (m^2 s^{-1})
e	Elementary Charge ($1.6 \cdot 10^{-19}$ Coulomb)
E_{act}	Activation energy (kJ/kmol)
F	Faraday Constant (C/mol)
$\Delta^r G$	Gibbs enthalpy of reaction (kJ/mol)
h	Enthalpy on a mole basis (kJ/kmol)
h	Enthalpy on a mass basis (kJ/kg)
H	Enthalpy (kJ)
I	Current (A)
i_0	Electric exchange current density (A)
i_1	Limiting current density (A)
K_{eq}	Equilibrium constant (-)
$\dot{m}$	Mass flow rate (kg/s)
$\dot{n}$	Molar flow (mol/s)
n_{cell}	Number of cell (-)
N_A	Avogadro Constant ($6.0 \cdot 10^{23}$ mol^{-1})
p_0	Standard pressure (bar)
p_i	Partial pressure (bar)
P	Electrical power output (kW)
Q	Heat (kJ)
R_u	Universal Gas Constant (8.31 J/(mol K)
R	Resistance (Ω)
T	Temperature (°C)
U_f	Utilization Factor (-)
V	Voltage (V)
W	Work (kJ)
W_{trev}	Reversible work transferred (kJ)
y	Molar fraction (-)

Abbreviations

AOR	Anode off-gas Recirculation
CGR	Cathode Gas Recycled
CHP	Combined Heat and Power
DORS	Degree Of Steam Reforming
ER	External Reforming
HHV	Higher Heating Value (kJ/kg)
HRSG	Heat Recovery Steam Generator
LHV	Lower heating Value (kJ/kg)
MSR	Methane Steam Reforming
NG	Natural Gas
OCV	Open Circuit Voltage (V)
SOFC	Solid Oxide Fuel Cell
WGS	Water Gas Shift

Greek

α	Charge transfer coefficient (-)
η	Efficiency (%)
ε	Porosity (-)
γ	Exchange current density (A m^{-2})
τ	Tortuosity (-)

Subscripts & Superscripts

act	Activation
anode	Anode
cathode	Cathode
conc	Concentration
eff	Effective
el	Electrical
F	Fuel
FC	Fuel cell
in	Inlet
inverter	Inverter
ohm	Ohmic
out	Outlet
parasitic	Parasitic
recycled	Recycled
rev	Reversible
stoich	Stoichiometry
th	Thermal
tot	Total

References

[1] Larminie, J., Dicks, A., Fuel Cell Systems Explained,

John Wiley & Sons Ltd., New York, 2000.

[2] Williams, M.C., 7th ed., Fuel Cell Handbook, EG&G Technical Services, Inc., 2004.

[3] Ozgoli, H.A., Ghadamian, H., Roshandel, R., Moghadasi, M., "Alternative Biomass Fuels Consideration Exergy and Power Analysis for a Hybrid System Includes PSOFC and GT Integration", Energy Sources, Part A: Recovery, Utilization, and Environmental Effects, 2015, 37: 1962-1970.

[4] Ozgoli, H.A., Ghadamian, H., Farzaneh, H. "Energy Efficiency Improvement Analysis Considering Environmental Aspects in Regard to Biomass Gasification PSOFC-GT Power Generation System", Procedia Environmental Sciences, 2013, 17: 831-841.

[5] Ghadamian, H., Hamidi, A.A., Farzaneh, H., Ozgoli, H.A., "Thermo-economic analysis of absorption air cooling system for pressurized solid oxide fuel cell/gas turbine cycle", Journal of Renewable and sustainable Energy, 2012, 4: 1-14.

[6] Ozgoli, H.A., Ghadamian, H., Hamidi, A.A., "Modeling SOFC & GT Integrated-Cycle Power System with Energy Consumption Minimizing Target to Improve Comprehensive cycle Performance (Applied in pulp and paper, case studied)", International Journal of Engineering Technology, 2012, 1: 1-6.

[7] Ozgoli, H.A., Moghadasi, M., Farhani, F., Sadigh, M. "Modeling and Simulation of an Integrated Gasification SOFC-CHAT Cycle to Improve Power and Efficiency", Environmental Progress & Sustainable Energy, 2017, 36: 610-618.

[8] Tsiakaras, P., Demin, A., "Thermodynamic analysis of a solid oxide fuel cell system fuelled by ethanol", Journal of Power Sources, 2010, 102: 210-217.

[9] Braun, R.J., Klein, S.A., Reindl, D.T., "Evaluation of system configurations for solid oxide fuel cell-based micro-combined heat and power generators in residential applications", Journal of Power Sources, 2005, 158: 1290-1305.

[10] Powell, M., Meinhardt, K., Sprenkle, V., Chick, L., McVay, G., "Demonstration of a highly efficient solid oxide fuel cell power system using adiabatic steam reforming and anode gas recirculation", Journal of Power Sources, 2012, 205: 377–384.

[11] Halinen, M., Rautanen, M., Saarinen, J., Pennanen, J., Pohjoranta, A., Kiviaho, J., Pastula, M., Nuttall, B., Rankin, C., Borglum, B., "Performance of a 10 kW SOFC Demonstration Unit", ECS Transactions, 2011, 35: 113–120.

[12] Halinen, M., Pohjoranta, A., Kujanpää, L., Väisänen, V., Salminen, P., "Summary of the RealDemo – project 2012-2014", VTT Technical Research Centre of Finland, 2014.

[13] Yakabe, H., Ogiwara, T., Hishinuma, M., Yasuda, I., "3-D model calculation for planar SOFC", Journal of Power Sources, 2001, 102: 144-154.

[14] Aguiar, P., Adjiman, C. S., Brandon, N. P., "Anode-supported intermediate temperature direct internal reforming solid oxide fuel cell. I: model-based steady-state", Journal of Power Sources 2004, 138: 120-136.

[15] Sanchez, D., Chacartegui, R., Munoz, A., Sanchez, T., "On the effect of methane internal reforming modelling in solid oxide fuel cells", International Journal of Hydrogen Energy, 2008, 33: 1834-1844.

[16] Al-Sulaiman, F. A., Dincer, I., Hamdullahpur, F., "Energy analysis of a trigeneration plant based on solid oxide fuel cell and organic Rankine cycle", International Journal of Hydrogen Energy, 2010, 35: 5104–5113.

[17] Meshcheryakov, V. D., Kirillov, V. A., Sobyanin, V. A., "Thermodynamic Analysis of a Solid Oxide Fuel Cell Power System with External Natural Gas Reforming", Theoretical Foundations of Chemical Engineering, 2006, 40: 51–58.

[18] Becker, W.L., Braun, R.J., Penev, M., Melaina, M., "Design and technoeconomic performance analysis of a 1 MW solid oxide fuel cell polygeneration system for combined production of heat, hydrogen, and power", Journal of Power Sources, 2012, 200: 34–44.

[19] Colson, C. M., Nehrir, M. H., "Evaluating the Benefits of a Hybrid Solid Oxide Fuel Cell Combined Heat and Power Plant for Energy Sustainability and Emissions Avoidance", IEEE Transactions on Energy Conversion, 2011, 26: 141-148.

[20] US Department of Energy, National Energy Technology Laboratory, and RDS, "Natural Gas-Fueled Distributed Generation Solid Oxide Fuel Cell Systems", 2009.

[21] Chick, L., Weimar, M., Whyatt, G., Powell, M., "The Case for Natural Gas Fueled Solid Oxide Fuel Cell Power Systems for Distributed Generation", Fuel Cells, 2015, 15: 49–60.

[22] Geerssen, T.M., "Physical properties of natural gases, Properties of Groningen Natural Gas", N.V. Nederlandse Gasunie, 1988, page 31.

[23] Haussinger, L.R., Watson, A., "UllmannÕs Encyclopedia of Industrial Chemistry. Wiley-VCH Verlag GmbH & Co.", Weinheim, Germany, http://www.wiley-vch.de, online edition, 2002.

[24] Hoogers, G., Fuel Cell Technology Handbook, chapter 5, The Fueling Problem: Fuel Cell Systems, CRC Press LLC, 2003.

[25] Rostrup-Nielsen, J.R., Sehested, J., Norskov, J.K., "Hydrogen and synthesis gas by steam and CO_2 reforming," Advances in Catalysis, 2002, 47: 65-139.

[26] Valenzuela, M.A., Zapata, B., Hydroprocessing of Heavy Oils and Residual, Taylor & Francis Group, LLC, 2007.

[27] Newsome, D.S., The water-gas shift reaction. Catalysis Reviews, 1980, Available in: http://dx.doi.org/10.1080/03602458008067535.

[28] Singhal, S.C., Kendall, K., High Temperature Solid Oxide Fuel Cells, Fundamentals, Design and Applications. ISBN: 1856173879. Elsevier, 2003.

[29] Bove, R., Ubertini, S., Modeling Solid Oxide Fuel Cells. Springer, 2008.

[30] O'Hayre, R.P., Cha, S.W., Colella, W., Prinz, F.B., Fuel Cell Fundamentals. ISBN: 0471741485. John Wiley & Sons, INC., 2006.

[31] Lisbona, P., Corradetti, A., Bove, R., Lunghi, P., "Analysis of a solid oxide fuel cell system for combined heat and power applications under non-nominal conditions," Electrochimica Acta, 2007, 53: 1920-1930.

[32] Toonssen, R., "Sustainable Power from Biomass, Comparison of technologies for centralized or de-centralized fuel cell systems", PhD thesis, TU Delft, 2010.

[33] Hazarika, M.M., Ghosh, S., "Simulated Performance Analysis of a GT-MCFC Hybrid System Fed with Natural Gas", International Journal of Emerging Technology and Advanced Engineering, 2013, 3: 292-298.